Available online at www.sciencedirect.com
SCIENCE DIRECT®
PERGAMON
Radiation Physics and Chemistry 68 (2003) 109–113
Radiation Physics and Chemistry
www.elsevier.com/locate/radphyschem

Particle-in-cell Monte Carlo (PIC-MC) simulations of plasma–wall interactions in low-pressure AR plasma

A. Cenian[a,*], A. Chernukho[b], C. Leys[c]

[a] *Institute of Fluid-Flow Machinery, Polish Academy of Sciences, Fiszera 14, Gdańsk 80-952, Poland*
[b] *Heat and Mass Transfer Institute, P. Brovki Street 15, Minsk 220072, Belarus*
[c] *Department of Applied Physics, RUG, B-9000 Gent, Rozier 44, Belgium*

Abstract

The 1d3v (1D in displacement and 3D in velocity space) PIC-MC model is used in this work in order to study the sheath formation and the ambipolar diffusion in low-pressure, small-diameter Ar discharge. The departure from plasma neutrality and its consequences are investigated. The Bohm criterion for a sheath formation is not fulfilled in the low range of Ar concentrations.

Keywords: Ar plasma; Bohm criterion; Plasma neutrality

1. Introduction

The low pressure Ar discharges are important, e.g. for efficient fluorescent lamp operation (Kawamura and Ingold, 2001). At the low pressure and small discharge-chamber diameters, i.e. when the rates of particle–wall collisions come close to the frequencies of bulk processes, the plasma–wall interactions become very important and could not be, a priori, neglected.

There are various approaches to investigate plasma–wall interactions. The fluid models are based on a solution of the Boltzmann (or its moments, i.e. continuity, momentum and energy conservation equations) and Poisson's equation. In the Particle-in-cell Monte Carlo (PIC-MC) models the Boltzmann equation and the averaging procedure using a derived EEDF is substituted by the numerical integration of observable along the particle trajectories. The collisions are treated here as instantaneous processes, governed by the probability law related to the measured cross sections.

The plasma–wall interactions have lately been investigated by using various PIC-MC models, e.g. Chabert and Sheridan (2000), Kono (2001) and Kawamura and Ingold (2001). For example, an important fundamental issue of multiple-sheath formation in electronegative discharges was discussed. Various assumptions were used in order to make the PIC-MC simulation feasible.

In the planar one-dimensional (1D) PIC-MC model of Chabert and Sheridan (2000) the trajectories of positive and negative ions are calculated, while the density of electrons is described by the Boltzmann distribution. At each time step, a fixed number of negative and positive ions are created—space-uniformly. The collisionless ions are lost either to the wall or in recombination processes described by the probability law.

Kono (2001) proposed a spherical 1d2v (1D displacement 2D velocity) PIC-MC model for the probe immersed in the plasma. The MC trajectories are calculated for all charged particle (including electrons), that gradually fill up the initially empty simulation box due to thermal particle flux from the ambient plasma. The particles passing the boundaries of the simulation box are lost (absorbed on the wall or diffused into the ambient plasma). All particles move in the electric field determined by the Poisson equation. The particle collisions (which include the charge transfer and ionization processes) are treated in a simplified manner, i.e. the velocity after the particle collision is replaced by the random thermal velocity corresponding to the

*Corresponding author.
E-mail address: cenian@imp.gda.pl (A. Cenian).

0969-806X/03/$ - see front matter
doi:10.1016/S0969-806X(03)00264-0

temperature of that specie ($T^+ = T^- = T_e/100$ is assumed).

Kawamura and Ingold (2001) has developed the most realistic, 1d3v (1D displacement 3D velocity) PIC-MC model for electropositive plasma of axis-symmetrical low-pressure systems. The axial component of charged-particles velocity introduced to the model enables determination of the self-sustained electric field by assuming that the electron ionization processes should balance electron losses (both in the plasma bulk and at the wall). The ambipolar diffusion as well as ionization, elastic and excitation processes are taken into account, while simulating electron trajectories. The charge transfer processes are considered, when ion trajectories are calculated. Already introductory investigations proved that this model could be used in order to study fundamental problems of plasma–wall interaction.

Therefore, the model of Kawamura and Ingold (2001)—after slight technical modifications—was used in this work in order to study thoroughly the problem of ambipolar diffusion and a sheath formation in low-pressure Ar discharges. The various assumptions used in fluid models, e.g. Boltzmann electrons, plasma neutrality, etc., were verified under the studied low-collisional conditions.

2. Model description

The Poisson equation is solved using the density of charged "quasi-particles" determined in grid points by calculation of MC trajectories. Each "quasi-particle" represents large number of electrons or Ar^+ ions moving in the electric field determined by a solution of Poisson's equation.

The low-pressure ($p \leqslant 1$ Torr) Ar-plasma of positive column, bounded by non-conducting wall of cylindrical geometry (tube radius $R = 1$ cm) is considered. A simulation box is divided by computational grid (250 grid points), with spacing separation decreasing inversely proportional to the distance from the (radial) symmetry axis ($\Delta r_i \sim 1/r_i$). The azimuthal symmetry and uniformity in axial direction is assumed, i.e. although MC trajectories are calculated in three dimensions only radial distribution of charged particle densities is considered in the 1D Poisson equation.

An assumed axial current, $I_z = 10$ mA, is sustained by the axial electric field ($E_z(r) = \text{const}$), i.e. it is derived by requirements that impact ionization rate equals the charge losses due to the plasma–wall interactions. When the electron balance is not fulfilled the E_z value is changed and the procedure is continued till the steady-state conditions are established. The neglect of other than direct-ionization processes severely limits the plasma concentrations of Ar discharges, which can be properly described, i.e. less than $10^{22}\,m^{-3}$ (Kawamura and Ingold, 2001). It corresponds to the pressure range $p < 41$ Pa, when gas (ion) temperature $T = 300$ K is assumed.

The Bessel profile is assumed as initial condition (it accelerates significantly the simulation procedure if compared to the uniform spatial profile), with arbitrary coordinates and velocities (fixed electron energy and thermal ion energy distribution). The MC trajectories for "super particles" are calculated using "null collision method" (Lin and Bardsley, 1977). Arbitrary collision frequency is chosen in such a way that the mean free path $\lambda_p < 0.002R$. It enables the correct inclusion of field evolution into the equation of motion. The calculation of trajectories is broken at the chosen time steps and the charged species concentration at the grid points is determined, in order to solve Poisson's equation. When the new radial potential and electric field is determined, the trajectory calculations are continued. The particles crossing the simulation-box boundary are removed from a simulation.

The ionization, elastic and excitation processes are taken into account while simulating electron trajectories. Charge-transfer processes are considered when ion trajectories are calculated (similar to L–K model described by Kawamura and Ingold, 2001). The cross sections for electron collisions are taken from Phelps (1999) database.

3. Results and discussion

Fig. 1 presents the profiles of charged-particle densities, kinetic energies, potential and electric field for different Ar densities ($[Ar] = 10^{20}$, 10^{21} and $10^{22}\,m^{-3}$). The results are close to these presented by Kawamura and Ingold (2001) for L–K cross section set—see their Fig. 7. The major differences are found for the lowest $[Ar] = 10^{20}\,m^{-3}$, e.g. the potential in the tube center is 25% lower than in Kawamura and Ingold (2001). Also, the calculated axial field, E_z, values, 78, 151 and 400 V/m for $[Ar] = 10^{20}$, 10^{21} and $10^{22}\,m^{-3}$, respectively, agree reasonably well, except for the first value (which is 35% lower). This may result from significantly larger cross section for electron impact ionization in the high-energy range in Phelps (1999) than in L–K set. Finally, the reasonably good agreement of the results Kawamura and Ingold (2001)—and so ours—with experimental data should be stressed.

The calculated potential at the wall (see Fig. 1d) is not equal to that determined by Lieberman and Lichtenberg (1994), i.e. $\varphi_w = -T_e/2\ln(M_i/2\pi m)$. The ratio $-\varphi_w/T_e$ was found at 2.19, 2.55 and 2.70 for Ar densities 10^{20}, 10^{21} and $10^{22}\,m^{-3}$, respectively. It is similar to the values of Kawamura and Ingold (2001) but it is much less than the theoretical 4.68 value of Lieberman and Lichtenberg (1994). This failure must be related to the assumption of

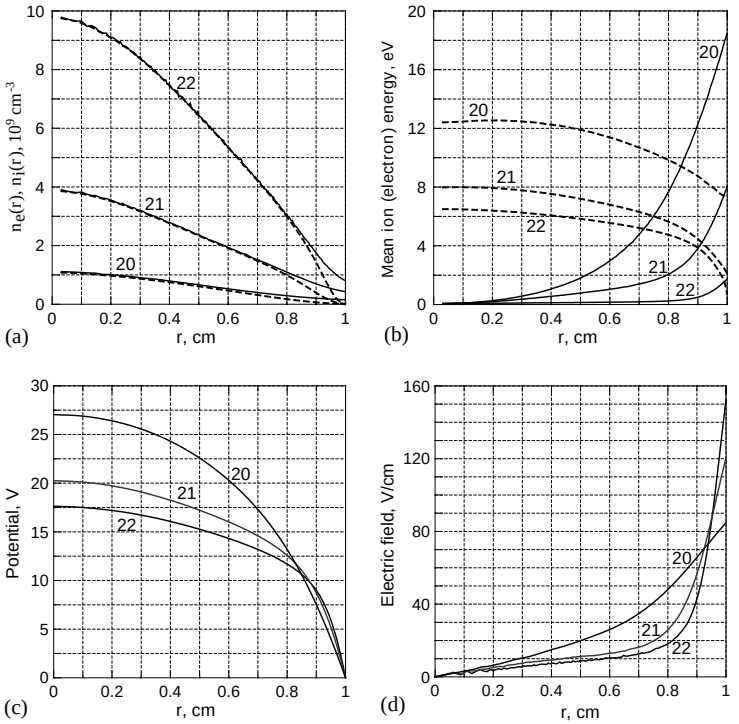

Fig. 1. Profiles of (a) charged-particle densities, (b) mean kinetic energies, (c) potential and (d) electric field for the chosen Ar densities: line 20–$10^{20}\,m^{-3}$, line 21–$10^{21}\,m^{-3}$, line 22–$10^{22}\,m^{-3}$. The dashed lines correspond to the electrons and solid lines to ions.

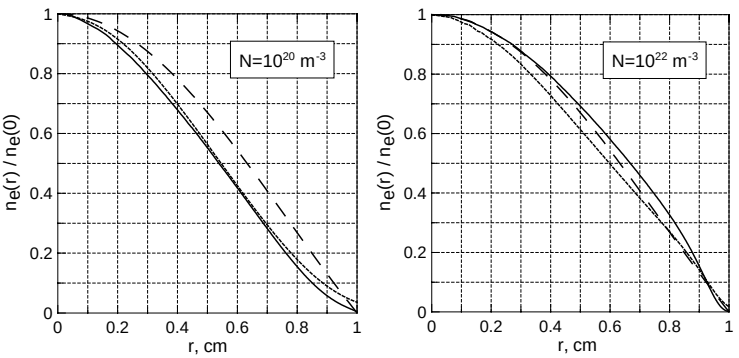

Fig. 2. Comparison of electron density profiles (solid line) with Boltzmann-electron (dotted line) and Bessel-function approximation (dashed line) for Ar densities 10^{20} and $10^{22}\,m^{-3}$.

constant flux in the sheath, which is not fulfilled here—see Fig. 4.

Fig. 2 presents comparison between the calculated electron density profile and the approximate density profiles: Boltzmann—$n(r) = n_0 \exp(e\varphi/kT_e)$ and (zero-order) Bessel function—$n(r) = n_0 J_0(2.404r/R)$, approximations. The first approximation corresponds to the assumption of non-collisional electrons, the second to the free electron diffusion in the cylindrical tube with electron-source along the symmetry axis. It is seen that the electron profile is well described by the "Boltzmann electron" approximation in the lowest considered range of [Ar]. When the Ar density is increased, the above approximation fails and the "free diffusion" approximation describes electron density profile better—see Fig. 2b.

The net charge profiles related to the average electron density $<n_e(r)>$ are shown in Fig. 3. It has been proved that in the studied (low) Ar concentration the plasma neutrality is not preserved even in the bulk plasma. The

thickness of the ion sheath, estimated by the distance from the point, where the flat profile of net charge ends, up to the wall, is 6, 3.5 and 2.5 mm or ~ 14, ~ 18 and $\sim 18\ \lambda_D$ for [Ar] $= 10^{20}$, 10^{21} and $10^{22}\,m^{-3}$, respectively. The Debye length λ_D was estimated for electron energies in the bulk plasma and is respectively equal to 0.44, 0.2 and 0.11 mm. It should be stressed here that the ion velocities, at the estimated sheath edges, do not fulfill Bohm criterion, i.e. $v_i \geqslant v_s$, where $v_s = (kT_e/\mu_i)$ is the ion-sound velocity. Surprisingly enough, in the case of highest considered [Ar] the averaged ion velocity is less than the ion-sound velocity in the whole discharge volume. This must be related to the failure of the neutrality condition—basic for Bohm criterion to be fulfilled (see e.g. Riemann, 1991), for the studied low-pressure Ar discharges.

Fig. 4a presents spatial profiles of electron and ion fluxes. Although ion-flux profiles oscillate, it can be seen that the condition $\Gamma_e \approx \Gamma_i$ is generally well preserved, i.e.

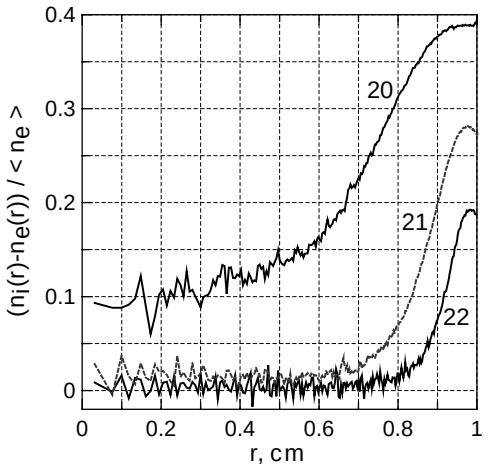

Fig. 3. Net-charge profile related to the mean electron density for the chosen Ar densities: line 20–$10^{20}\,m^{-3}$, line 21–$10^{21}\,m^{-3}$, line 22–$10^{22}\,m^{-3}$.

the charge redistribution is accomplished. The fluxes are not monotonic functions of Ar concentration. The particle flux at each point increases as [Ar] grows from 10^{20} to $10^{21}\,m^{-3}$ and later drops as concentration increases to $10^{22}\,m^{-3}$. It might be, however, easily checked that the frequency of electron-diffusion losses (which depend inverse proportional to the Ar density) monotonic decreases with the [Ar], as is to be expected.

Fig. 4b presents the ratios $\Gamma_i/\nabla n_i$ (smooth curves) or $\Gamma_e/\nabla n_e$ (erratic ones). The values related to ambipolar diffusion coefficients are far from constant and differ for electron and ions, especially at the sheath region. This is again related to the fact that the neutrality conditions, $n_e = n_i$, is not preserved in the sheath zone. Therefore, the well-known relation $D_a = (\mu_i D_e + \mu_e D_i)/(\mu_i + \mu_e)$ should be replaced by

$$D_{ai} = (\mu_i \nabla n_e/\nabla n_i D_e + \mu_e n_e/n_i D_i)/(\mu_i + \mu_e n_e/n_i)$$

for ions (for electrons one should exchange the indexes "i" and "e"), where both n_e/n_i and $\nabla n_e/\nabla n_i$ are functions of radial coordinate r in the sheath zone (see Fig. 2a). However, the $\Gamma_e/\nabla n_e(r)$ and to lesser degree $\Gamma_i/\nabla n_i(r)$ are not constant even in the bulk plasma region (at least in the region of considered low and high Ar concentrations). This may be related to relatively small tube diameter—less than the electron mean free path λ_e for low [Ar]. The values of λ_e of order of 11, 1 and 0.12 cm were determined, for [Ar] $= 10^{20}$, 10^{21} and $10^{22}\,m^{-3}$, respectively. This could not, however, explain the $\Gamma_e/\nabla n_e(r)$ variation in the high concentration range.

The ambipolar diffusion coefficient estimated from the slow varying region $r < 0.4R_0$ is equal to ~ 11, ~ 8.0 and $\sim 3.2\,m^2/s$ for Ar concentrations equal to 10^{20}, 10^{21} and $10^{22}\,m^{-3}$, respectively.

4. Conclusions

The generally accepted assumption about the plasma neutrality is not always fulfilled under low-pressure Ar

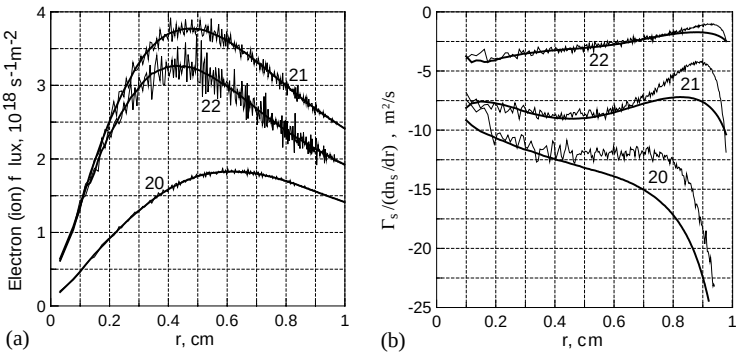

Fig. 4. Profiles of (a) charged particles fluxes and (b) $\Gamma_s/\nabla n_s(r)$ for the chosen Ar densities: line 20–$10^{20}\,m^{-3}$, line 21–$10^{21}\,m^{-3}$, line 22–$10^{22}\,m^{-3}$. The smooth curves correspond to positive ions ($s = i$) and erratic ones to electrons ($s = e$).

discharge conditions. The departure from quasi-neutrality increases with the pressure fall at least in the considered pressure range, $0.41 < p < 41$ Pa. The failure of plasma-neutrality assumption influences the plasma–wall interactions, e.g. the Bohm criterion at the sheath edge must not be fulfilled. Also, the ambipolar diffusion coefficient becomes space dependent in the sheath zone.

The Boltzmann electron approximation describes the electron profile well only in the lowest studied [Ar] range. As the concentration increases the electron profile is much better described by the free electron diffusion approximation with electron source at the symmetry axis.

The ambipolar diffusion coefficients were determined and were found to be monotonous decaying with a pressure growth in the considered [Ar] range. The sheath thickness decays with Ar concentration quite similar to the Debye lengths.

Acknowledgements

We acknowledge financial support from the bilateral Belgium-Polish cooperation program and the Project 4T10B 01922 of Polish Committee for Scientific Researches.

References

Chabert, P., Sheridan, T.E., 2000. Kinetic model for a low pressure discharge with negative ions. J. Appl. Phys. 33, 1854–1860.

Kawamura, E., Ingold, J.H., 2001. Particle in cell simulations of low pressure small radius positive column discharges. J. Phys. D 34, 3150–3163.

Kono, A., 2001. Complex sheath formation around the spherical electrode in electronegative plasma: a comparison between fluid and a particle simulation. J. Phys. D 34, 1083–1090.

Lieberman, M.A., Lichtenberg, A.J., 1994. Principles of Plasma Discharges and Materials Processing. Wiley-Interscience Publication, Wiley, New York.

Lin, S.L., Bardsley, J.N., 1977. Monte Carlo simulation of ion motion in drift tubes. J. Chem. Phys. 66, 435–445.

Phelps, A.V., 1999. The cross section available on ftp://jila.colorado.edu/collision.data, unpublished.

Riemann, K.-U., 1991. The Bohm criterion and sheath formation. J. Phys. D 24, 493–518.